



RESEARCH ARTICLE

Synthesis and Optical Studies of $\text{La}_{1.1}\text{Ti}_{1-x}\text{W}_x(\text{O,N})_3$ Prepared by Sol-Gel Methodology.

Narendra G. Sarda^{1*}, Takanori Hayashi¹, Andrew Chan², Yuta Takeuchi¹, Kyosuke Harada¹, Kei-Ichiro Murai¹, Geoffrey I.N. Waterhouse², Toshihiro Moriga¹

1. Graduate School of Advanced Technology and Science, Tokushima University, 2-1 Minami-Josanjima, Tokushima 770-8506, Japan.
2. School of Chemical Sciences, The University of Auckland, Private Bag 92019, New Zealand.

Manuscript Info**Manuscript History:**

Received: 15 November 2015
Final Accepted: 26 December 2015
Published Online: January 2016

Key words:

LaTiO_2N , Perovskite,
Oxynitride, Ammonolysis,
Tungsten,

***Corresponding Author**

Narendra G. Sarda.

Abstract

Perovskite-type oxynitride having general formula $\text{La}_{1.1}(\text{Ti}_{1-x}\text{W}_x)(\text{O,N})_3$ with different compositions ($X = 0.01, 0.02, 0.03, 0.04, 0.05$) were synthesized by a thermal ammonolysis of oxide precursors prepared via a sol-gel method. The products formed with different composition were systematically characterized by XRD, SEM-EDS, particle size distribution analysis, UV-vis and oxygen/nitrogen analysis. Scanning electron microscopy (SEM) showed morphological changes of the microstructure with increasing tungsten content. UV-visible reflectance spectra showed that absorption edge wavelengths of the oxynitrides were in the range of 545nm – 575 nm, corresponding to the bandgap energy of 2.28eV – 2.16eV. Among all $\text{La}_{1.1}(\text{Ti}_{1-x}\text{W}_x)(\text{O,N})_3$ compositions ($X = 0.03$) showed the highest redshift with decreasing band gap.

Copy Right, IJAR, 2016. All rights reserved.

Introduction:-

Perovskite-type oxynitrides are promising materials showing the potential application in many fields such as, harmless inorganic pigments (Jansen et al., 2000, Aguiar et al., 2008, Chen et al., 2015), Phosphors for LED (Xie et al., 2013 and Sarda et al., 2016), Visible light photocatalysis (Maegali et al., 2014), gas sensor and dielectric materials. Different kinds of oxynitrides have been synthesized in the past decades and their applications are also developing in various fields (Xie et al., 2013).

Inorganic pigments with harmless elements showed its promising replacements of the toxic (e.g. Pb, Cd, HgS) pigments. Especially, inorganic non-toxic red pigments are commercially high in demand due to their wide applicability. However, Fe_2O_3 has been widely used as an ecofriendly inorganic red pigment, but due to the unsatisfactory colour performance there is need to develop alternative pigment. A number of interesting approaches have been done and continued to elaborate alternative, low cost, non-toxic and satisfactory colour performance for the paint and desk-jet printing application (N. Imanaka et al., 2014, Maegali et al., 2014, Moriga et al., 2006 & 7, Masuda et al., 2009 a, b, and Sarda et al., 2015)

LaTiO_2N oxynitrides are of special interest due to their variety of attractive characteristics in this regards. In earlier studies, LaTiO_2N pigments showing Orange, green, yellow and blue colours have been synthesized by controlling anion stoichiometry and nitrating conditions (Moriga et al., 2006). We have also reported that slight excess of titanium over lanthanum result in the deterioration of the reflectivity is attributable to the increase ratio of Ti^{3+} compared to Ti^{4+} .

In this context, different compositions of perovskite-type oxynitride $\text{La}_{1.1}(\text{Ti}_{1-x}\text{W}_x)(\text{O,N})_3$ were synthesized and optical studies has been done. Due to their low cost and high coloration efficiency WCl_6 used as a doping material

(Sun et al., 2014 and Maegli et al., 2014). The aim of this study was to investigate the effect of tungsten doping on the optical properties of LaTiO_2N and in an attempt to produce vivid red pigments.

Material and Methods:-

Materials:-

$\text{La}(\text{NO}_3)_3 \cdot 6\text{H}_2\text{O}$, titanium isopropoxide, ethylene glycol, citric acid and WCl_6 were obtained from Wako Pure Chemical Industries, Ltd., Japan were used as starting materials. Ammonia gas was obtained from sumitomo Seika Chemicals Co., Ltd., Japan.

Thermal ammonolysis experiments:-

A series of five different compositions of perovskite-type $\text{La}_{1.1}(\text{Ti}_{1-x}\text{W}_x)(\text{O,N})_3$, ($X = 0.01, 0.02, 0.03, 0.04, 0.05$) powders were prepared via a sol-gel method with subsequent nitridation by thermal ammonolysis. First, $\text{La}(\text{NO}_3)_3 \cdot 6\text{H}_2\text{O}$ (2.381g, 0.0055mol) and titanium isopropoxide (1.279g, 0.0045mol) were added to ethylene glycol (24.7g) at room temperature with constant stirring. WCl_6 were dissolved in ethanol (20g) and then added into the above solution. A molar excess of La relatively to Ti was taken.

Citric acid (19.1g) and distilled water (20g) were then added to give a homogeneous solution. More details were described in reference (Sarda et al., 2015). Further, prepared precursor was heated under a NH_3 flow of $1\text{dm}^3/\text{min}$ for 5h at 950°C . After the nitridation was complete, the product was cooled down to room temperature in the furnace. Throughout these experiments, the amount of Lanthanum nitrate hexahydrate was fixed and the molar ratio of the cations (lanthanum, titanium and tungsten) was according to $\text{La/Ti/W} = 1.1/1-x/x$, where the value of x was changed to obtain the desired substitution levels.

Product characterization:-

Phase purity was checked by X-ray diffraction (Rigaku Smart lab X-ray diffractometer). The incident X-rays had a wavelength of 1.5406\AA ($\text{Cu-K}\alpha$). XRD data was recorded over the 2θ range $20-80^\circ$ operated at 40 kV and 150 mA. Phase identification was made with reference to the JCPDS database. Optical diffuse reflectance spectra were measured with a double beam spectrometer (JASCO V-550DS). The La:Ti ratio of the products was determined by XRF. Anion contents were determined by the hot gas extraction method using a Horiba EMGA-920 analyzer (O/N analyzer). For the analysis, the sample was accurately weighed into a graphite crucible with Ni-Sn as flux and then heated to 3000°C . Oxygen in the sample was converted into CO while nitrogen evolved in its molecular form. The amount of both gases was determined using infrared and thermal conductivity detectors. Particle size distribution of the oxynitride sample was measured by laser diffraction particle size analyzer (Microtrac HRA X-100). Morphologies and particle size were also evaluated by SEM (Philips XL-30 field emission gun scanning electron microscope). Secondary electron detectors coupled with EDS (Energy-Dispersion Spectroscopy). The SEM-EDS provides detailed imaging information about the morphology and surface texture of individual particles, as well as elements composition of the samples. A relatively low acceleration voltage of 15 kV was used (Lu et al., 2004). Specimens were mounted on black carbon tape and platinum sputter coated for analysis. The surface distributions were collected from SEM images using different magnifications.

Result and Discussion:-

Phase composition of $\text{La}_{1.1}(\text{Ti}_{1-x}\text{W}_x)(\text{O,N})_3$ powders :-

The powder X-ray diffraction patterns of the $\text{La}_{1.1}(\text{Ti}_{1-x}\text{W}_x)(\text{O,N})_3$, shown in Fig.1, revealed that all the samples could be assigned to the single phase of the perovskite. No indications for impurity phases were found with increasing doping amount of tungsten. An expansion of the unit cell parameters with increasing tungsten content was observed as a shift of the peak position of the reflections towards lower 2θ angles. Fig.2 shows that the volume of the unit cell indeed increases with increasing tungsten content. The structural refinements were calculated by CellCalc Ver.2.20 software.

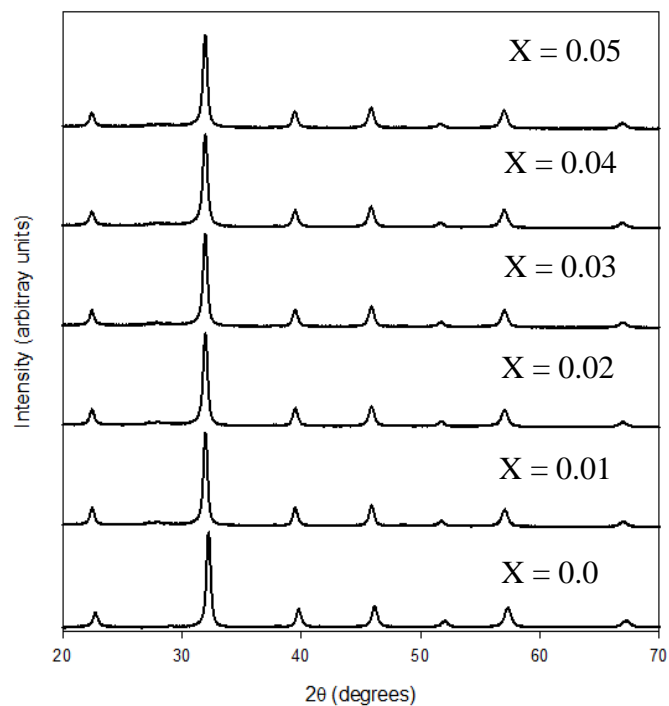


Fig.1 X-ray powder diffraction patterns of the $\text{La}_{1.1}(\text{Ti}_{1-x}\text{W}_x)(\text{O,N})_3$ powders.

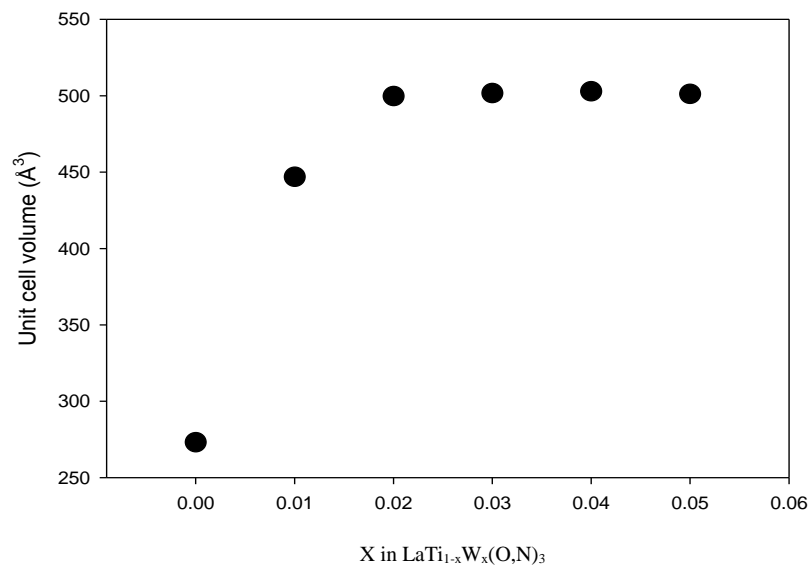








Fig.2 Unit cell volume of the W^{6+} content in $\text{La}_{1.1}(\text{Ti}_{1-x}\text{W}_x)(\text{O,N})_3$ powders.

Table 1 Summarized physical and optical data for $\text{La}_{1.1}\text{Ti}_{1-x}\text{W}_x(\text{O},\text{N})_3$ powders

Sample	Mean particle size (μm)	O (wt.%)	N (wt.%)	O/N	Composition	Colour	E_g (eV)
X = 0.0	8.62	16.11	3.74	3.77	$\text{LaTi}(\text{O}_{0.79}\text{N}_{0.21})_{2.97}$		2.28
X = 0.01	2.83	15.91	3.31	4.21	$\text{La}_{1.1}\text{Ti}_{0.99}\text{W}_{0.01}(\text{O}_{0.81}\text{N}_{0.19})_{3.12}$		2.19
X = 0.02	3.54	16.81	2.87	5.13	$\text{La}_{1.1}\text{Ti}_{0.98}\text{W}_{0.02}(\text{O}_{0.84}\text{N}_{0.16})_{3.2}$		2.18
X = 0.03	2.81	16.73	3.42	4.5	$\text{La}_{1.1}\text{Ti}_{0.97}\text{W}_{0.03}(\text{O}_{0.82}\text{N}_{0.18})_{3.27}$		2.16
X = 0.04	4.64	16.43	3.45	4.17	$\text{La}_{1.1}\text{Ti}_{0.96}\text{W}_{0.04}(\text{O}_{0.81}\text{N}_{0.19})_{3.25}$		2.19
X = 0.05	1.81	15.94	3.2	4.35	$\text{La}_{1.1}\text{Ti}_{0.95}\text{W}_{0.05}(\text{O}_{0.81}\text{N}_{0.19})_{3.1}$		2.18

Particle size of the $\text{La}_{1.1}(\text{Ti}_{1-x}\text{W}_x)(\text{O},\text{N})_3$ powders :-

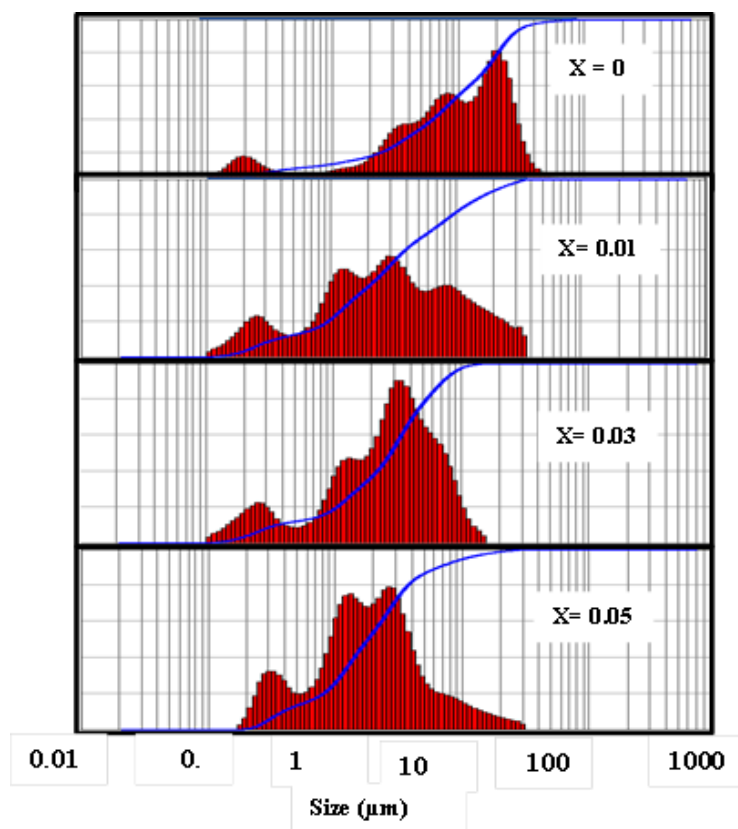


Fig.3 Particle size distributions of $\text{La}_{1.1}\text{Ti}_{1-x}\text{W}_x(\text{O},\text{N})_3$ where X= 0, 0.01,0.03 and 0.05 respectively

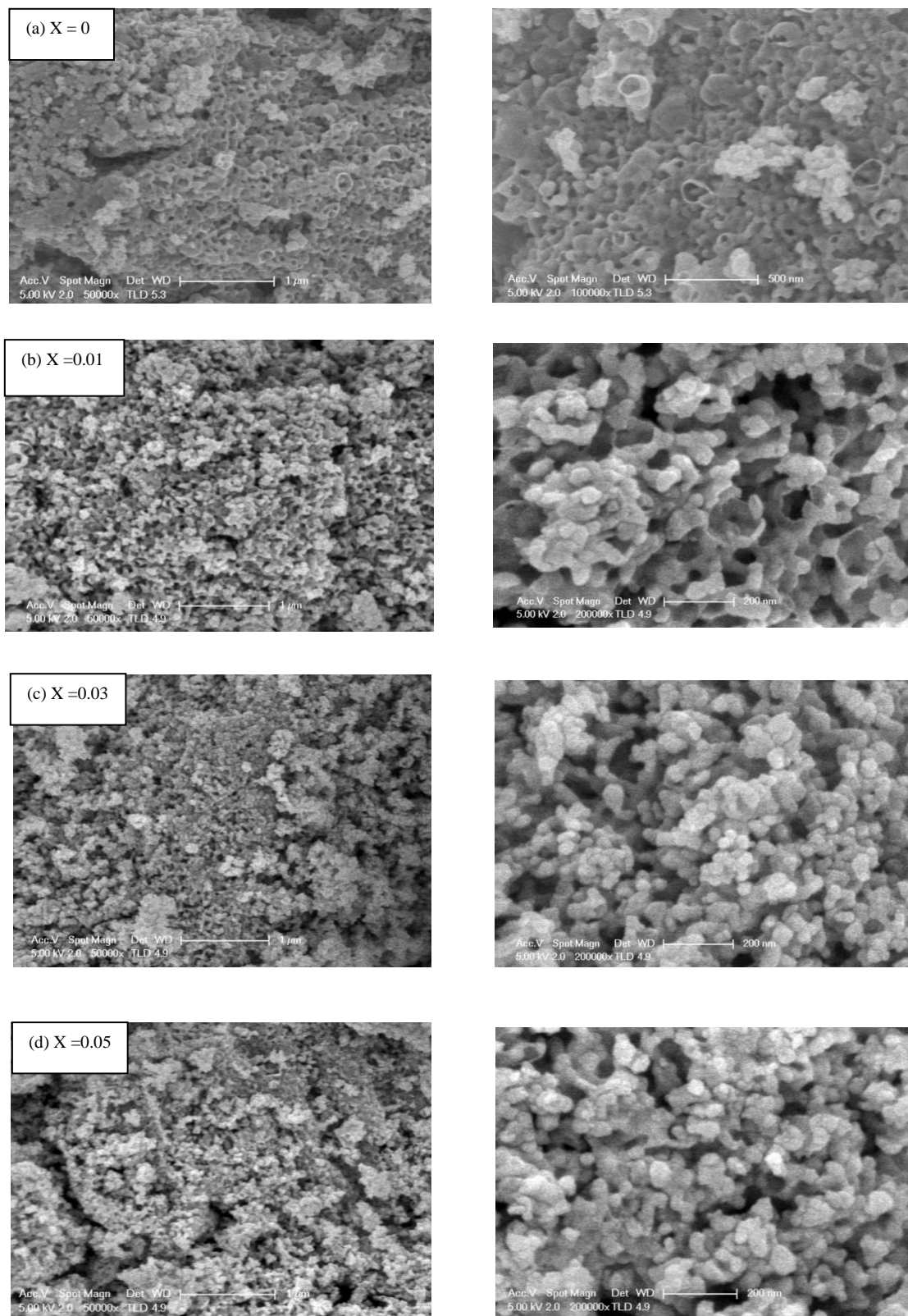


Fig.4. Scanning electron microscopy (SEM) micrographs of $\text{La}_{1.1}(\text{Ti}_{1-x}\text{W}_x)(\text{O,N})_3$ powders, where (a) $x=0$, (b) $x=0.01$, (c) $x=0.03$ and (d) $x=0.05$ respectively

The particle size distribution of the $\text{La}_{1.1}(\text{Ti}_{1-x}\text{W}_x)(\text{O,N})_3$ powders with different compositions is shown in Fig.3. Median particle sizes are summarized in Table 1. The median particle size of the LaTiO_2N powder was $8.622\mu\text{m}$ in the absence of W^{6+} . Tungsten doping reduces the median particle sizes to $<4\mu\text{m}$. SEM images of the $\text{La}_{1.1}(\text{Ti}_{1-x}\text{W}_x)(\text{O,N})_3$ where ($X= 0, 0.01, 0.03$ and 0.05) are shown in Fig. 4 respectively. SEM confirmed a decrease in particle size when tungsten doping and excess of La relative to Ti was used in the oxynitride powders (Maegali et al., 2014). From Fig.4 (b), (c) and (d) it can be observed that, with an increase in the tungsten doping amount from $X=0.01$ to 0.05 , the number of the dispersed particles increased and the finely powdery particles were seen.

Optical properties of the $\text{La}_{1.1}\text{Ti}_{1-x}\text{W}_x(\text{O,N})_3$ powders :-

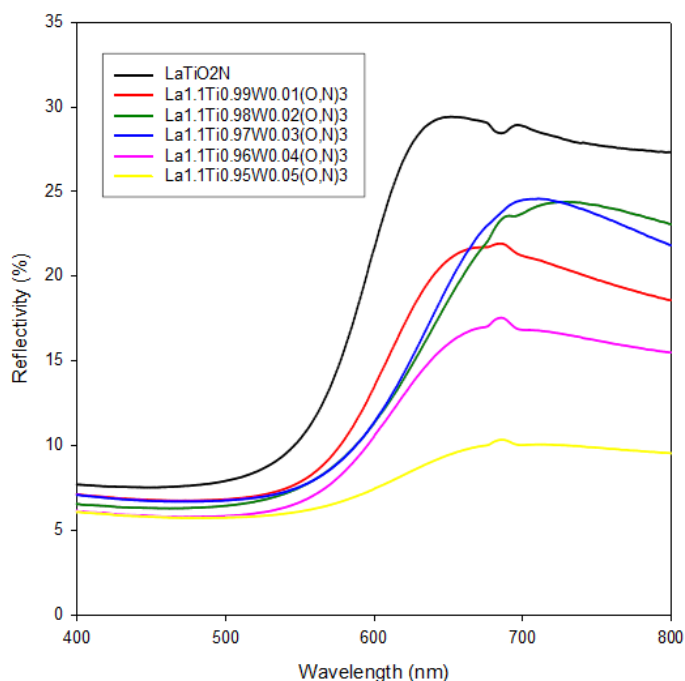


Fig.5 UV-vis reflectance spectra for $\text{La}_{1.1}(\text{Ti}_{1-x}\text{W}_x)(\text{O,N})_3$

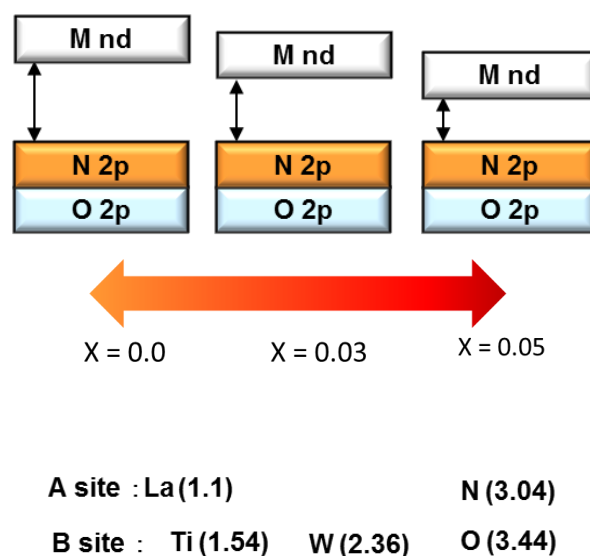


Fig.6 schematic sketch of electronegativity of the B cation on the optical band gap in oxynitride perovskite

The UV-vis absorption spectra of the oxynitride are shown in Fig.5. In order to compare the absorption edges between the crystalline non doped LaTiO_2N and tungsten doped $\text{La}_{1.1}(\text{Ti}_{1-x}\text{W}_x)(\text{O,N})_3$. Precursors which were prepared for the comparison with their corresponding oxynitrides, showed band gaps $<3\text{eV}$. This value is higher than the visible light energy, which can explain colourlessness. The optical absorption edge of the LaTiO_2N had a cut-off at 545 nm , which corresponds to an optical band gap of 2.28 eV . The optical absorption edge of the W^{6+} doped $\text{La}_{1.1}(\text{Ti}_{1-x}\text{W}_x)(\text{O,N})_3$ was extended to 575 nm , which is equivalent to an optical band gap of 2.16 eV . The absorption edge shifts to longer wavelengths due to their narrower band gaps. This result cannot be illustrated by atomic bond distance values, because W^{6+} and Ti^{4+} have almost the same ionic radius (0.60 \AA and 0.605 \AA) in an octahedral coordination. (Aguilar et al., 2008 and Maegli et al., 2014) have claimed that, redshift and/or color changes are not only due to the nitrogen content, but also from different electronegativities of the B cations. The influence of different electronegativities of the B cations is schematically shown in Fig.6. Figure shows that as tungsten content increases, the electronegativity of the B cation increases and it is attributed to a decrease in band gap and/or redshift (Maegli et al., 2014).

The powder prepared at $\text{La}_{1.1}\text{Ti}_{0.95}\text{W}_{0.05}(\text{O,N})_3$ was reddish-brown in color with a median particle size $<2\mu\text{m}$ (Table 1), showed low reflectivity above the absorption edge (Fig.5) due to the presence of a mixed valent state.

for Ti^{3+}/Ti^{4+} . However, in our previous work we have reported that, when the oxynitrides contained more titanium than stoichiometric composition, resulting in deterioration of reflectivity in the longer wavelengths of the absorption edge and showed the darkening in the colour. Inversely, the oxynitride contained excess of La relative to Ti can endure without affecting the optical properties (Masuda et al., 2009 ,b, and Sarda et al., 2015) .

Spectra EDS of $La_{1.1}Ti_{1-x}W_x(O,N)_3$ powders :-

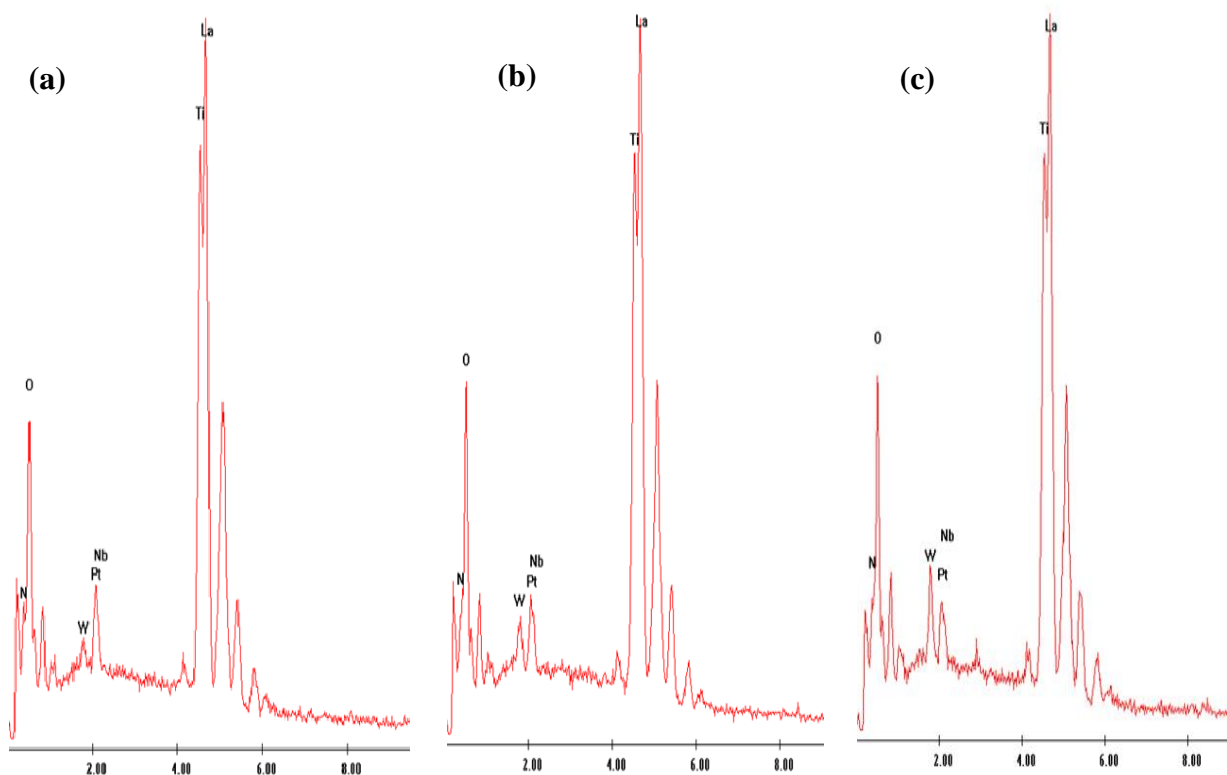


Fig.7. EDS spectra of (a) $La_{1.1}Ti_{0.99}W_{0.01}(O,N)_3$, (b) $La_{1.1}Ti_{0.97}W_{0.03}(O,N)_3$ and (c) $La_{1.1}Ti_{0.95}W_{0.05}(O,N)_3$

Table 2. Elemental composition of $La_{1.1}Ti_{1-x}W_x(O,N)_3$ measured by EDS

Sample	Element Atomic Weight							
	La	Ti	O	N	Nb	W	Pt	Total
$La_{1.1}Ti_{0.99}W_{0.01}(O,N)_3$	11.8	9.1	50.5	27.2	0	0.5	0.9	100
$La_{1.1}Ti_{0.98}W_{0.02}(O,N)_3$	11.4	8.4	53.3	25.4	0	0.6	0.9	100
$La_{1.1}Ti_{0.97}W_{0.03}(O,N)_3$	12.7	9.2	50.8	25.3	0	1	1	100
$La_{1.1}Ti_{0.96}W_{0.04}(O,N)_3$	12.3	9	51.2	25.4	0	1.2	0.9	100
$La_{1.1}Ti_{0.95}W_{0.05}(O,N)_3$	12.7	9.4	49.4	26	0	1.5	1	100

Fig.7 shows the elemental composition of $\text{La}_{1.1}\text{Ti}_{1-x}\text{W}_x(\text{O},\text{N})_3$, where, ($X= 0.01,0.03$ and 0.05) were studied by Energy-dispersion spectrometer (EDS) respectively. La, Ti, O and N were found as main elements. Platinum (Pt) was also detected which arises due to platinum coating were used for SEM observation. The elemental compositions obtained by EDS in the (Table 2) evidence of nitrogen deficiency in all the composition. It has been already reported by (Maegli et al., 2014) the presence of oxygen-rich intermediate-phases on atomic scale and without periodic ordering is possible; therefore such intermediate phases are not detectable by XRD (Aguiar et al., 2008). Results from Table 1 showed O/N ratio gradually increases with increasing tungsten content. This phenomenon is attributed to the difference in electronegativity between oxygen and nitrogen. The substitution of nitrogen by oxygen, a more electronegative element, involves an increase in ionicity of the bonding.

Conclusion:-

Different compositions of perovskite-type $\text{La}_{1.1}\text{Ti}_{1-x}\text{W}_x(\text{O},\text{N})_3$ were synthesized by thermal ammonolysis of oxide precursor prepared by a sol-gel method. There were no deterioration was seen with excess of La on the structural and optical properties of the oxynitride. No impurities were detected by XRD. Appropriate doping of W^{6+} and excess of La relative to Ti in the oxynitride allowed red-shifting of the absorption edge. UV-visible diffuse reflectance spectra showed the bandgap in the range of 2.28 eV- 2.16 eV $\text{La}_{1.1}\text{Ti}_{1-x}\text{W}_x(\text{O},\text{N})_3$. Colour of the pigment strongly depends on the light reflection from their surface and materials near inside the surface would hardly contribute to the colour. Therefore, excess of La in the given composition and very small amount of tungsten is fruitful way to increase the brightness of the oxynitride samples. Further work is focused on the XPS and crystal structure of the $\text{La}_{1.1}\text{Ti}_{1-x}\text{W}_x(\text{O},\text{N})_3$ in order to conclude the relationship with its body colour.

Acknowledgements:-

This work was partly supported by grant-in-aids from NEDO Industrial Technology Research Grant Program and the JSPS KAKENHI Grant-in-Aid for Scientific Research ©.

References :-

1. Jansen, M., Letschert, H.P. 2000. Inorganic yellow-red pigments without toxic metals. *Nature*; 404:980–982.
2. Aguiar, R., Logvinovich, D., Weidenkaff, A., Rachel, A., Reller, A., Ebbinghaus, S.G. 2008. The vast colour spectrum of ternary metal oxynitride pigments. *Dyes Pigm*; 76:70–75.
3. Chen, D., Habu, D., Masubuchi, Y., Torii, S., Kamiyama, T., Kikkawa, S. 2015. Partial nitrogen loss in SrTaO_2N and LaTiO_2N oxynitride perovskites. *Solid State Sciences*; 2015.08.18.
4. Xie, R., Hintzen, H.T. Bert. 2013. Optical properties of (oxy)nitride materials: a review. *J. Am. Ceram. Soc.*, 96 (3): 665-687.
5. Sarda, N. G., Fujigaki, H., Ogita, Y., Chan, A., Murai, K., Waterhouse, G. I. N. and Moriga T. 2016. Photoluminescence Properties of $(\text{Ba}_{1-(x+y)}\text{Sr}_x\text{Eu}_y)_2\text{Si}_6\text{O}_{12}\text{N}_2$ Phosphors for White LED Applications. *J. Nano Res.*, 36: 1-7.
6. Wendusu, Masui, T., Imanaka, N. 2014. Novel environment-friendly inorganic red pigments based on $(\text{Bi}, \text{Er}, \text{Y}, \text{Fe})_2\text{O}_3$ solid solutions. *J. As. Ceram Soc.*, 2: 195–198.
7. Sun, S., Masubuchi, Y., Motohashi, T., Kikkawa, S. 2014. Direct synthesis of nearly single-phase BaTaO_2N and CaTaO_2N powders. *J. Eur. Ceram. Soc.*, 35 (12).
8. Ozkan, E., Tepehan., F.Z. 2001. Optical and structural characteristics of sol-gel-deposited tungsten oxide and vanadium-doped tungsten oxide. *Sol. Energy Mater. Sol. Cells*; 68:265-277
9. Maegli, A. E., Sagarna, L., Populoh, S., Penkala, B., Otal, E. H., Weidenkaff, A. 2014. Optical and transport properties of $\text{LaTi}_{1-x}\text{M}_x(\text{O},\text{N})_{3+\delta}$ ($x=0; 0.1, \text{M}=\text{Nb}^{5+}, \text{W}^{6+}$) thin films prepared by plasma ammonolysis. *J. Solid State Chem.*, 211:106–112.

10. Masuda, Y., Mashima, R., Yamada, M., Ando, H., Kawasaki, T., Murai, K. and Moriga, T. 2009. 'a' Optical properties of (La,Sr)TiO₂N series depending on nonstoichiometries and particle sizes varying in accordance with heat treatment conditions. *Mater. Sci. and Eng.*, 1: 012018.
11. Masuda, Y., Mashima, R., Ikeuchi, K., Murai, K., Waterhouse, G.I.N., Metson, J.B., Moriga, T. 2009. 'b' Relationship between anion and cation nonstoichiometries and valancestate of titanium in perovskite-type oxynitrides LaTiO₂N. *J.Ceram. Soc. Jpn.*,117:76–81.
12. Moriga, T., Ikeuchi, K., Mashima, R., Aoki, D., Murai, K. 2007. Influence of cation nonstoichiometry on the optical properties of the perovskite-type oxynitrideLaTiO₂N. *J. Ceram. Soc. Jpn.*, 115(10):601–3.
13. Moriga, T., Aoki, D., Nishida, Y., Kitaji, K., Takahara, K., Murai, K. 2006. Blue-shift of absorption edge in LaTiO₂N by controlling the anion nonstoichiometry. *Phys. Stat. Sol. (a)*; 203(11):2818–22.
14. Sarda, N. G., Omune, M., Hayashi, T., Chan, A., Kataoka, S., Murai, K., Waterhouse, G. I.N., Moriga, T. 2015.
15. Structural and optical properties of perovskite-type LaTiO₂N synthesized using urea or thiourea as co-nitriding agents. *J. Eur. Ceram. Soc.*, 35 : 3311–3317.
- 16.
17. Lu, J., Rozgonyi, G., Rand, J., Jonczyk, R. 2004. Secondary phase inclusions in polycrystalline sheet silicon. *J. Crys. Gro.*, 269:599–605.
18. Aguiar, R., Kalytta, A., Reller, A., Weidenkaff, A. and Ebbinghaus, S. G. 2008. Photocatalytic decomposition of acetone using LaTi(O,N)₃ nanoparticles under visible light irradiation. *J. Mater. Chem.*, 18: 4260-4265.